

## Supporting Info

### **Electrochemical conversion of a bio-derivable hydroxy acid to a drop-in oxygenate diesel fuel**

Jérôme Meyers,<sup>\*,a</sup> Joel B. Mensah,<sup>\*,a</sup> F. Joschka Holzhäuser,<sup>a</sup> Ahmad Omari,<sup>b</sup> Christian C. Blesken,<sup>c</sup> Till Tiso,<sup>c</sup> Stefan Palkovits,<sup>a</sup> Lars M. Blank,<sup>c</sup> Stefan Pischinger,<sup>b</sup> Regina Palkovits<sup>\*,a</sup>

<sup>a</sup> Institut für Technische und Makromolekulare Chemie, RWTH Aachen University, Worringerweg 2, 52074 Aachen, Germany.

<sup>b</sup> Lehrstuhl für Verbrennungskraftmaschinen, RWTH Aachen University, Forckenbeckstraße 4, 52074 Aachen, Germany.

<sup>c</sup> Institut für Angewandte Mikrobiologie, RWTH Aachen University, Worringerweg 1, 52074 Aachen, Germany.

<sup>\*</sup> These authors contributed equally to this work.

<sup>\*</sup> author of correspondence: [palkovits@itmc.rwth-aachen.de](mailto:palkovits@itmc.rwth-aachen.de)

## **Table of Contents**

### **1 Experimental section**

Materials

HAA synthesis

Composition of simulated fermentation broth

Electrolysis

NMR

HPLC

Gas chromatography

Gas chromatography-mass spectrometry

Determination of the product yields

Determination of the fuel properties

### **2 Results**

Electrolysis in fermentative medium

Proposed reaction pathway

### **3 Analytical data**

### **4 References**

## 1 Experimental section

### Materials

3-Hydroxy decanoic acid ( $\geq 95\%$ ; 007Chemicals), methanol ( $\geq 99.8\%$ , TH-Geyer), ethanol ( $\geq 99.9\%$ ; TH-Geyer), acetonitrile ( $\geq 99.9\%$ , Roth), ethyl heptanoate (99%, Sigma-Aldrich), heptane ( $\geq 96\%$ , Sigma-Aldrich), potassium hydroxide ( $\geq 99.5\%$ ; Roth), tetrabutylammonium perchlorate (99%, Sigma-Aldrich), tetrabutylammonium tetrafluoroborate (99%, Sigma-Aldrich), trimethylamine ( $\geq 99.5\%$ , Roth), 1-nonanol (98%, Sigma-Aldrich), 2-nonanol (99%, Sigma-Aldrich), 2-nonanone ( $\geq 99\%$ , Sigma-Aldrich), nonanal (95%, Sigma-Aldrich), nonanal dimethyl acetal ( $>97\%$ , TCI), methyl nonanoate ( $>96\%$ , TCI) and nonane ( $\geq 99\%$ , Honeywell) were used as purchased without any further purification.

A custom-built electrolysis cell was used, which consisted of a small vial ( $V = 5 \text{ mL}$ ) with a 3D-printed support, to which both electrodes were attached, based on inexpensive and inert CPE (co-polyester) material. The distance between the electrodes was kept constantly at 3 mm, whereas the electrode surface in the solution was  $1 \text{ cm}^2$  for each electrode. The electrodes were fittingly sliced and smoothed or replaced after a series of reactions. A graphite anode and a titanium cathode were applied for the electrolysis of 3-hydroxy decanoic acid (3-HDA).

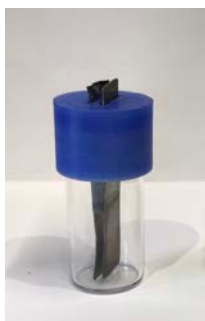


**Figure S1.** Illustration of a typical electrolysis cell setup with 3D-printed cap (out of CPE).

### HAA synthesis

For HAA synthesis, the recombinant *Pseudomonas taiwanensis* VLB120 pSB01 was cultivated in 2 L Fernbach shake flasks, filled with 500 mL lysogeny broth (LB) medium and 50 mg/L kanamycin. The cultivation was carried out for 4 days with a daily addition of 10 mL of a 50 % (w/v) glucose solution. The temperature was maintained at 30 °C and the flasks were shaken at 250 rpm with a shaking diameter of 50 mm. After the cultivation, the fermentation broth (FB) was heated up to over 100 °C for sterilization and enzyme denaturation. In the following, the FB was centrifuged and the supernatant was filtered.

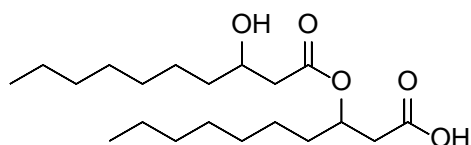


**Figure S2.** Molecular structure of 3-(3-hydroxy-alkanoyloxy)alkanoic acid (C10-C10).

### Composition of simulated fermentation broth

2 mL solution, 0.1 M 3-HDA, 0.1 M KOH, 80 mg  $\text{L}^{-1}$  HAAs,  $\text{KH}_2\text{PO}_4$  (388 g  $\text{L}^{-1}$ ),  $\text{NaH}_2\text{PO}_4$  (212 g  $\text{L}^{-1}$ ), 1 g  $\text{L}^{-1}$  EDTA and 10 g  $\text{L}^{-1}$   $\text{MgCl}_2$ .

## Electrolysis

The electrolysis experiments were conducted using a *Metrohm Autolab* PGSTAT 302N potentiostat or a *BASETech* BT-305 power unit. The program *Metrohm Nova* recorded the generated potential during the electrolysis measurement.

0°C cooling of the electrochemical cell in an ice bath was mandatory due to the increasing temperature of the reaction solution. The used equipment for electrolysis is described in the materials section above. The kinetic reactions had to be carried out individually as no samples could be taken from the cell as this would have considerably disturbed the equilibrium of the reaction in this small volume ( $V = 2\text{ mL}$ ). For each of the reported measurements, triplicate experiments were conducted under identical conditions.

## NMR

All  $^1\text{H}$  and  $^{13}\text{C}$  NMR spectra were measured at 25 °C with a *Bruker Avance* spectrometer at 400 and 100 MHz respectively. Approximately 20 mg of each substance were solved in  $\text{CDCl}_3$  (99.8%) and referenced to the residual solvent. The purity of the 3-HDA substrate as well as its conversion was analysed with  $^1\text{H}$  and  $^{13}\text{C}$  NMR spectroscopy.

**$^1\text{H}$  NMR (400 MHz,  $\text{CDCl}_3$ ):**  $\delta = 4.09\text{--}3.98$  (m, 1H), 2.64–2.30 (m, 2H), 1.67–1.08 (m, 12H), 0.94–0.79 (m, 3H) ppm.

**$^{13}\text{C}$  NMR (100 MHz,  $\text{CDCl}_3$ ):**  $\delta = 177.3$  (s), 68.1 (s), 41.0 (s), 36.7 (s), 31.9 (s), 29.6 (s), 29.4 (s), 25.6 (s), 22.8 (s), 14.2 (s) ppm.

## HPLC

The aqueous phase was analysed via high-performance liquid chromatography (*Shimadzu Prominence LC-20 system*) equipped with a RI detector and a *Macherey Nagel-Nucleodur* C18 Gravity column. The samples were eluted at 40 °C with a 70:30 (vol.%) mixture of acetonitrile and 0.2 wt.% aqueous formic acid using a flow rate of  $1.0\text{ mL min}^{-1}$ .

## Gas chromatography

After completion of each electrolysis experiment the mixture was acidified and extracted with 1 mL  $\text{H}_2\text{O}$  and 2 mL heptane. The products of the organic phase were quantified using a *Thermo Scientific Chromatograph Trace GC Ultra* equipped with a CP-WAX-52 (60m) column. Every sample contained 15 mg of ethyl heptanoate as internal standard and 1 mL heptane as solvent.  $\text{N}_2$  was used as carrier gas with a constant flow rate of approximately  $1.5\text{ mL min}^{-1}$  along with an inlet temperature of 250 °C and a split flow of  $50\text{ mL min}^{-1}$ . A temperature program of 70 °C (5 min) and 200 °C (15 min) with a heating ramp of  $8\text{ °C min}^{-1}$  was used for the analysis of 1  $\mu\text{L}$  of the sample.

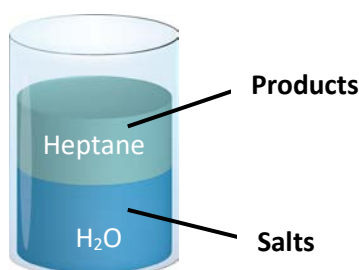


**Figure S3.** Schematic illustration of the extraction prior to the GC analysis.

## Gas chromatography-mass spectrometry

Measurements were carried out on a Varian CP-3800 gas chromatograph equipped with a CP-WAX-52 column (60 m x 250  $\mu\text{m}$  x 0.25  $\mu\text{m}$ ) and a Varian 1200L Quadrupole MS/MS fitted with an electron ionization (EI) source. The volume of injected sample was 1  $\mu\text{L}$  (diluted in methanol 1:10) and the GC signal was recorded with a flame ionization detector (FID). The EI voltage was set at 70 eV with a transfer capillary temperature of 250  $^{\circ}\text{C}$  and an ion source temperature of 250  $^{\circ}\text{C}$ .

## Determination of the product yields

### Liquid phase

As no products were detected in the aqueous phase using NMR and HPLC, the product yield in the organic phase represents the total yield of the products in the liquid phase, which was calculated as follows:

$$Y_{i,lp} = \frac{n_i}{n_0} * 100\%$$

where  $Y_{i,lp}$  is the yield of product  $i$  in the liquid phase in %,  $n_i$  the amount of substance  $i$  in the liquid phase in mol,  $n_0$  the initial amount of the substrate 3-hydroxy decanoic acid in mol. The respective values for  $n_i$  were determined using gas chromatography.

### Gas phase

The determination of the gaseous product fraction was significantly more challenging. In the employed open cell set-up, it was not possible to collect the gaseous phase. Electrolysis reactions under pressure in general need to be carried out with caution as the explosion limits of the evolving oxyhydrogen gas must be considered. To this day, no commercial electrolysis cells are available for this type of experiments.

To approximate the product yield of the gas fraction, we designed a novel pressurised cell that can withstand internal pressures of >5 bar with a volume of 15 mL (see Figure S4 below). The cell is divided into two chambers, one containing the electrolyte solution and the other one being used to continuously cool the neighboring chamber. The products are then collected in a directly linked gasbag, which was subsequently analysed using offline GC and MS. The hydrogen amount was measured with a quadrupole mass spectrometer (CIRRUS 2 device by MKS Instruments), equipped with a combined faraday cage and electron multiplier detector. The remaining gaseous products were identified by gas chromatography on an Agilent HP6890 system with a 2 m Shin carbon ST 100/120 mesh micro-packed column and a TCD detector.



**Figure S4.** Newly designed pressurised cell for exemplary analysis of the gaseous phase.

The yield of the products in the gas phase ( $\text{CO}$ ,  $\text{CO}_2$ ,  $\text{CH}_4$ ) were calculated as follows:

$$Y_{i,gp} = \frac{n_i}{n_0} * 100\%$$

We have performed an electrolysis experiment under similar conditions (0.1 M 3-HDA and 0.1 M KOH, 15 mL solution,  $j = 0.1 \text{ A cm}^{-2}$ , C and Ti electrodes with surfaces of  $10 \text{ cm}^2$ ) as in our smaller open cell setup. However, the same efficiencies could not be achieved since it was not possible to adapt all reaction parameters to this novel setup. Beyond that, the *in-situ* extraction of the absorbed  $\text{CO}_2$  out of the organic solvent (MeOH) was the biggest challenge. In this regard, elevated internal temperatures were necessary, which could be achieved by operating the reaction cell without cooling. Unfortunately, this often lead to spillage of the reaction solution in the attached hose, making reproducibility subject to a substantial error. Significant amounts of  $\text{CO}_2$  (77% yield) were obtained by conducting the reaction with 12 Farad eq. since the reaction temperature inside the cell otherwise was too low. The obtained gaseous products for this reaction are listed in Table S2 together with the yields of the C9-based products of the liquid phase (for the open cell setup). Thereby, an approximation for the actual carbon balance could be provided. For each of the remaining reaction time points, where no gas fraction could be quantitatively determined, the 3-HDA conversion was slightly (ca. 5-10%) above the overall C9 based product yield of the organic phase, meaning that the carbon balance could be closed to a high degree (90-95%).

Noteworthy, the determination of the yield for  $\text{CO}_2$  and  $\text{H}_2$  was expected to be subject to error as the formation of these gases may also arise from an oxidation of the solvent ( $\text{MeOH}$  being oxidised to  $\text{CO}_2$  and  $\text{H}^+$  being reduced to  $\text{H}_2$ ). This was also confirmed for the herein used conditions as conducting the electrolysis of neat MeOH without substrate (only 0.1M KOH in MeOH,  $0.1 \text{ A cm}^{-2}$ ) showed a significant conversion of MeOH into  $\text{CO}_2$  and  $\text{H}_2$ . However, this phenomenon is expected to be less pronounced with the presence of the substrate (3-HDA) as the anodes are primarily blocked by the substrate oxidation, thus less MeOH is oxidized.

In theory,  $\text{CO}_2$  and  $\text{H}_2$  are formed during (non-)Kolbe electrolysis in a 2:1 ratio. However, with the aforementioned solvent oxidation an accurate quantification of the respective ratio originating from the substrate 3-HDA is not possible.

The analysis of the obtained gas mixture for 3-HDA electrolysis in the novel setup (Figure S2) showed that 1.63 mmol  $\text{CO}_2$  and 18.24 mmol  $\text{H}_2$  are present in the gas phase, corresponding to a ratio of 1:11. The comparatively high amount of  $\text{H}_2$  might be rooted in the superior solubility of  $\text{CO}_2$  in MeOH.

#### Faraday efficiency

The Faraday efficiency  $\varepsilon$  is proportional to the amount of electrons  $z$ , that took part in the product formation, divided by the charge  $Q$  that passed between the electrodes during the experiment and calculates as follows:

$$\varepsilon = \frac{z * \sum n_i * F}{Q} * 100\%$$

where  $\sum n_i$  describes the total molar amount of the electrochemically formed products and  $F$  the Faraday constant ( $96485.33 \text{ C mol}^{-1}$ ).

#### **Carbon balance of the 3-HDA electrolysis**

In order to determine the overall carbon balance, the gaseous products were also taken into consideration (see Table S2). However, the yields for the C1 products, especially  $\text{CO}_2$ , must be treated with great caution due to the fact that  $\text{CO}_2$  also originates from the simultaneous oxidation of MeOH and can also partially dissolve in methanol. Furthermore, over-oxidation of the non-Kolbe products is highly probable at such an elevated number of Farad equivalents. It was however only possible to extract significant amounts of  $\text{CO}_2$  by conducting the reaction with 12 Farad eq. since the reaction temperature inside the cell was otherwise too low and thereby the  $\text{CO}_2$  solubility in MeOH, too high.

**Table S1.** Overall yields for the products in gas and liquid phase for the reaction conducted over 12 Farad eq. (0.1 M 3-HDA and 0.1 M KOH,  $j = 0.1 \text{ A cm}^{-2}$ , C and Ti electrodes)

[%]	CH <sub>4</sub>	CO <sub>2</sub>	CO	Nonane	2-Nonanone	Nonanal	1-Nonanol	Nonanal dimethyl acetal	Methyl nonanoate	$\Sigma$
<b>Gaseous product yield (C1)*</b>	1.4	76.6	13.0	-	-	-	-	-	-	<b>91.0</b>
<b>Liquid product yield (C9 based)**</b>	-	-	-	9.5	25.8	18.1	3.7	11.0	18.7	<b>87.7</b>
<b>Conversion</b>	-	-	-	-	-	-	-	-	-	<b>100</b>

\* The gaseous fraction was collected in a pressurised cell setup ( $V = 15 \text{ mL}$ ).

\*\* The yield in the organic phase is the total yield in the liquid phase (no water-soluble products).

Closing the carbon balance for experiments conducted in fermentation broth displayed to be more challenging, since already after the first 10 minutes of reaction time in the diluted fermentation broth, 3-HDA conversions (measured with HPLC method) above 75% were achieved with non-Kolbe product yields of less than 20%. This is rooted in the fact that a high amount of non-identifiable side products are generated in the fermentative medium, which makes a closed carbon cycle in this environment not possible.

**Table S2.** Overall yield in liquid phase and 3-HDA conversion at each measured reaction time point in MeOH

Reaction time [min]	10	20	30	60	120
Overall product yield in liquid phase [%]	71	88	95	91	86
3-HDA conversion [%]	79	93	98	100	100

Noteworthy, the highly excessive amount of Farad charge eq. after 30 minutes (3 Farad eq.) is believed to lead to an over-oxidation of the non-Kolbe products, explaining the slight decrease in yields after reactions times greater than 30 min.

### Determination of the fuel properties

To determine the fuel properties, reagent grade samples of the various product components shown in Figure 3a were purchased and then mixed to produce the expected C9-oxygenate. The components were mixed according to the volume fractions given in Table S1. The latter also shows the method used to determine the respective property.

**Table S3.** Overview of the components of the tested C9 mixture and corresponding method used for the determination of the respective fuel property

Line	Property	Unit	C9-oxygenate	Nonane	2-Nonanone	Nonanal	1-Nonanol	Nonanal dimethyl acetal	Methyl nonanoate	Analytical method
1	CAS Nr.	-	-	111-84-2	821-55-6	124-19-6	143-08-8	18824-63-0	1731-84-6	-
2	Molecular formula	-	-	C <sub>9</sub> H <sub>20</sub>	C <sub>9</sub> H <sub>18</sub> O	C <sub>9</sub> H <sub>18</sub> O	C <sub>9</sub> H <sub>20</sub> O	C <sub>11</sub> H <sub>24</sub> O <sub>2</sub>	C <sub>10</sub> H <sub>20</sub> O <sub>2</sub>	-
3	Volume fraction	-	-	0.09	0.269	0.191	0.036	0.281	0.133	Predefined based on Fig. 3a
4	Density at 15°C	kg m <sup>-3</sup>	0.834	0.718	0.83	0.827	0.828	0.85	0.9	Measured according to DIN EN ISO 12185
5	Mass fraction in C9-Fuel	-	-	0.077	0.268	0.189	0.036	0.286	0.143	Calculated from line 3 and 4
6	Oxygen mass fraction	-	0.13	0	0.113	0.113	0.111	0.170	0.186	Calculated according to line 2
7	Hydrogen mass fraction	-	0.13	0.156	0.127	0.127	0.139	0.128	0.116	Calculated according to line 2
8	Carbon mass fraction	-	0.74	0.844	0.761	0.761	0.750	0.702	0.698	Calculated according to line 2
9	Lower heating value	MJ kg <sup>-1</sup>	36.91	-	-	-	-	-	-	Measured according to DIN 51900-2
10	Lower heating value at 15°C	MJ L <sup>-1</sup>	30.79	-	-	-	-	-	-	Calculated from line 4 and 9
11	Specific carbon content	g MJ <sup>-1</sup>	20.1	-	-	-	-	-	-	Calculated from line 8 and 9
12	Derived cetane number	-	63	-	-	-	-	-	-	Measured according to DIN EN 15195
13	Flash point	°C	58.5	-	-	-	-	-	-	Measured according to DIN EN ISO 2719
14	Vapor pressure	mbar	< 7	5.9	2.133	0.66	0	0.3	0.26	Estimation based on vapor pressures of mixture components
15	Boiling point / distillation range	°C	150-213	150	195	191	211	213	210	Estimation based on boiling point of mixture components
16	Cold filter plugging point	°C	-24							Measured according to DIN EN 116
17	Kinematic viscosity	mm <sup>2</sup> s <sup>-1</sup>	1.4	-	-	-	-	-	-	Measured according to DIN EN ISO 3104



## 2 Results

### Electrolysis in fermentative medium

Three different ratios of FB to MeOH (1:1, 1:2 and 15:85) were studied for the direct 3-HDA electrolysis in the fermentation medium. The results are compared to a reference experiment of the respective solvent composition with pure 3-HDA as substrate. After 10 minutes (1 Farad eq.) of electrolysis, yields of maximal 15% were achieved in fermentative medium, which is comparatively low compared to the values reached in the water/MeOH mixture (15:85) and in solely MeOH. Given that the 15:85 FB/MeOH mixture displayed the most satisfying option, a reaction time course was drawn in this medium (Fig. 3b), demonstrating that substantially higher yields (up to 61%) can be achieved after an extended amount of Farad equivalents.

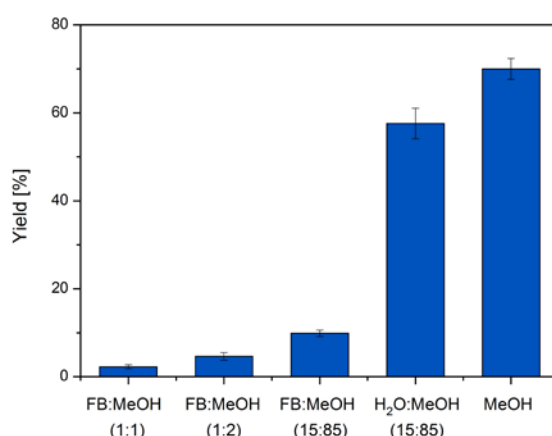
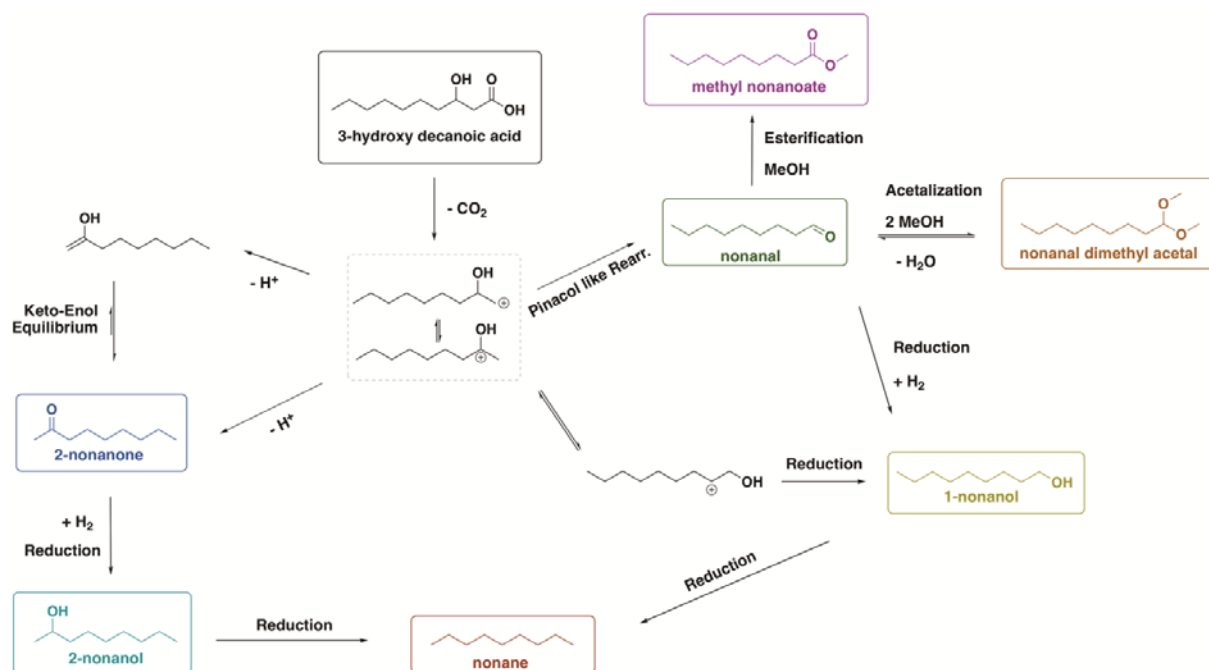


**Figure S5.** Comparison of the overall yield in different reaction media after 10 minutes (1 Farad eq.) of 3-HDA electrolysis (with FB = fermentation broth). Conditions: 0.1 M 3-HDA and 0.1 M KOH, 2 mL solution,  $j = 0.1 \text{ A cm}^{-2}$ , C and Ti electrodes.

### Proposed reaction pathway

First, anodic decarboxylation of 3-HDA leads to the formation of a  $\beta$ -hydroxy carbocation, which is deprotonated to 1-nonen-2-ol, which rapidly forms 2-nonanone (due to keto-enol tautomerization). Alternatively, the pinacol-pinacolone like rearrangement of the alkyl chain to the formed  $\beta$ -hydroxy carbocation may also lead to nonanal. The affinity for migration induced by the rearrangement of the carbocation for non-Kolbe electrolysis of  $\beta$ -hydroxy carboxylic acids was extensively described by Shono *et al.*<sup>1</sup> The generated nonanal may undergo solvolysis with MeOH leading to the formation of the nonanal dimethyl acetal. This mechanism is strongly supported by the formation of nonanal diethyl acetal when EtOH was used as solvent. Noteworthy, according to literature acetal formation typically occurs in acidic medium and does not occur in a basic environment.<sup>2,3</sup> Yet, the anode might shift the pH locally to lower values leading to an increased number of protons and an acid catalyzed acetalization. This phenomenon was already thoroughly described by the groups of Harnisch and Nyberg.<sup>4,5</sup>

Esterification of nonanal with the solvent MeOH yielding methyl nonanoate was also observed. The electrocatalytic esterification of an aldehyde has been previously reported in literature by Finney *et al.*<sup>6</sup> On the cathode side, both nonanal and 2-nonanone are reduced to 1-nonanol or 2-nonanol, respectively, as no membrane separation was employed. A further reduction of these alcohols generates fully deoxygenated nonane.



Scheme S1. Proposed reaction paths to the seven detected non-Kolbe products in KOH and MeOH.

### 3 Analytical data

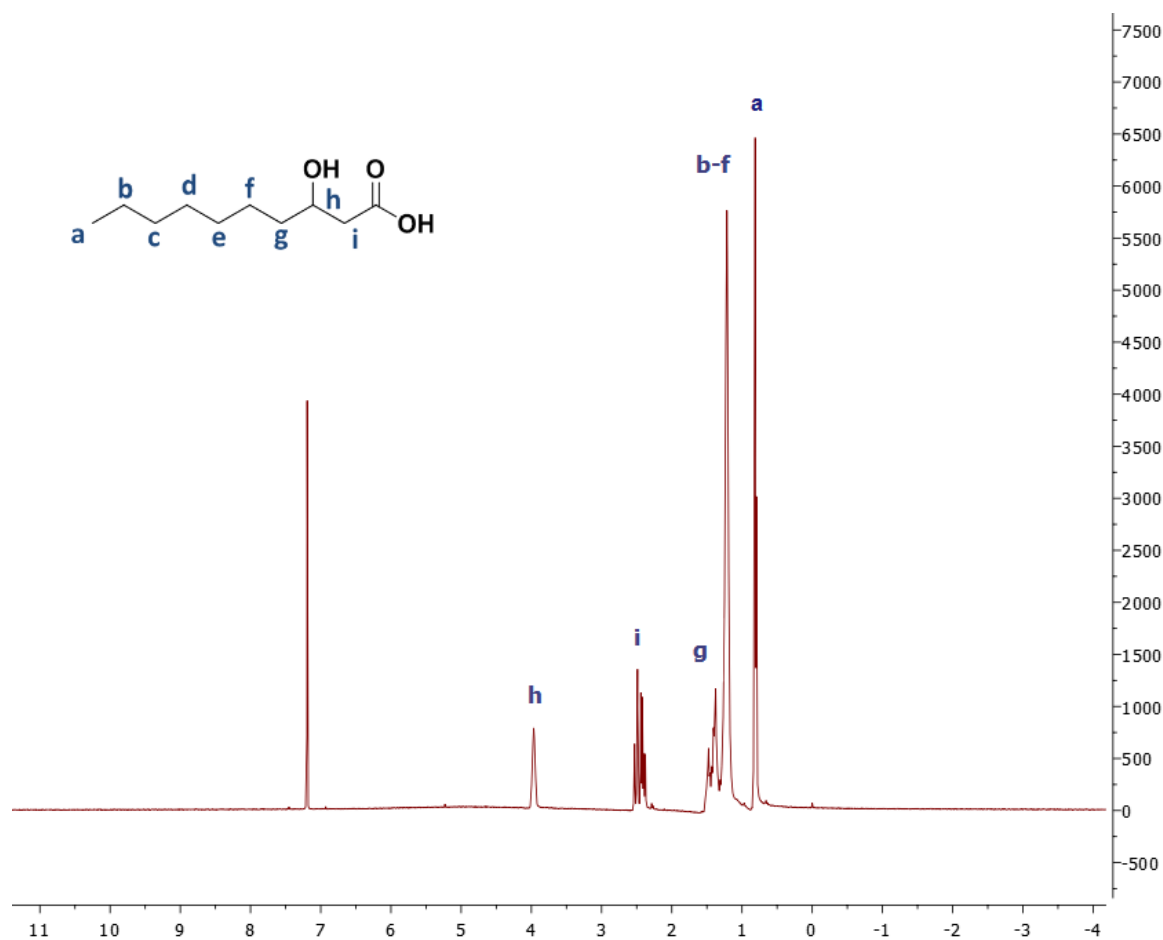


Figure S6.  $^1\text{H}$  NMR spectrum of the applied 3-hydroxy decanoic acid.

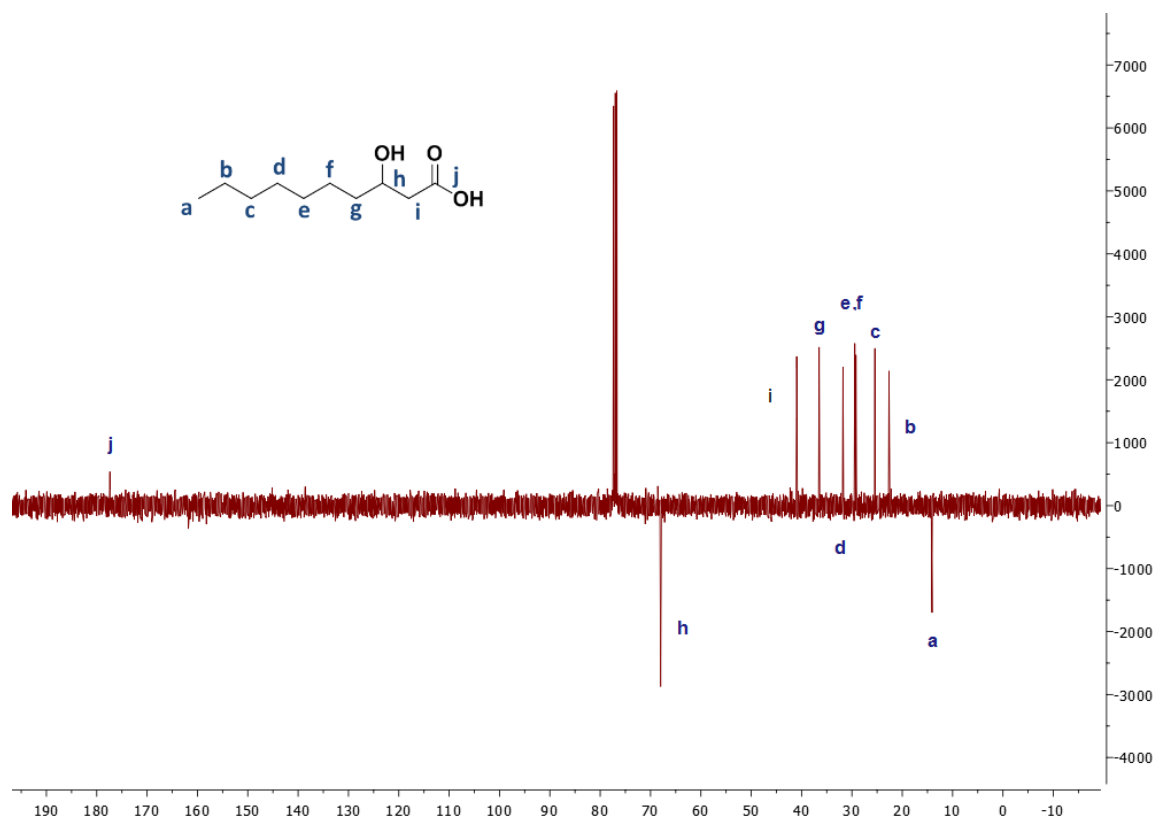


Figure S7.  $^{13}\text{C}$  NMR spectrum of the applied 3-hydroxy decanoic acid.

## 4 References

- 1 T. Shono, J. Hayashi, H. Omoto and Y. Matsumura, *Tetrahedron Lett.*, 1977, **18**, 2667–2670.
- 2 G. W. Meadows and B. de B. Darwent, *Can. J. Chem.*, 1952, **30**, 501–506.
- 3 F. A. Carey and R. J. Sundberg, *Advanced Organic Chemistry Part A: Structure and Mechanisms*, Springer, New York, 5th edn., 2007, vol. 5.
- 4 C. Stang and F. Harnisch, *ChemSusChem*, 2016, **9**, 50–60.
- 5 L. Eberson and K. Nyberg, 1976, pp. 1–129.
- 6 E. E. Finney, K. A. Ogawa and A. J. Boydston, *J. Am. Chem. Soc.*, 2012, **134**, 12374–12377.